



Adsorptive removal of nitrate ions from aqueous solution using modified biodegradable-based hydrogel

M.A. Abdel Khalek^a, Ghada A. Mahmoud^{b,*}, Eman M. Shoukry^c, M. Amin^c,
Aya H. Abdulghany^c

^aCentral Metallurgical Research and Development Institute, (CMRDI) P.O. Box 87, Helwan, Cairo, Egypt,
email: kalekma@yahoo.com (M.A.A. Khalek)

^bNational Center for Radiation Research and Technology, Atomic Energy Authority, P.O. Box 29, Nasr City, Cairo, Egypt;
Tel. +2-01065495895; Fax: +2-022 2749298; email: ghadancrrt@yahoo.com (G.A. Mahmoud)

^cFaculty of Science, Al-Azhar University, Nasr City, Cairo 11371, Egypt, emails: eman_shoukry2002@yahoo.com (E.M. Shoukry),
nemo131998@gmail.com (M. Amin), ayahussien32@gmail.com (A.H. Abdulghany)

Received 30 August 2018; Accepted 8 March 2019

ABSTRACT

This study aims to remove nitrate (NO_3^-) ions from aqueous solutions using biodegradable-based adsorbents. For this purpose (Chitosan/Gelatin/2-(N,N-Dimethylamino) ethyl methacrylate) (Cs/GltN/PDMAEMA) hydrogel was prepared by gamma irradiation. The prepared hydrogel was modified using thiourea by converting the hydroxyl groups into thiol groups to form (Cs/GltN/PDMAEMA)-treated. Moreover, the SiO_2 trapped in Cs/GltN/PDMAEMA hydrogel to perform Cs/GltN/PDMAEMA/ SiO_2 composite was also prepared. The swelling behavior of the prepared adsorbents was studied as functions of time and pH. Batch adsorption experiments were performed to study the effects of various operating parameters such as initial pH, contact time, initial ions concentration and temperature on the adsorption of NO_3^- ions. The result showed that the best adsorption capacity was obtained at pH 2 within 100 min and the optimum sorbent dosage was 10 g/L. The adsorption capacities were ordered in sequence of Cs/GltN/PDMAEMA/ SiO_2 composite followed by Cs/GltN/PDMAEMA-treated then Cs/GltN/PDMAEMA hydrogel. The rates of adsorption were found to follow the pseudo-second-order model. It was found that Freundlich's equation fits the adsorption better than the Langmuir's equation. The free energy of adsorption (ΔG°), enthalpy (ΔH°), and entropy (ΔS°) changes were calculated to predict the nature of adsorption.

Keyword: Adsorption; Composite; Hydrogel; Nitrate removal; Water treatment

1. Introduction

The extensive use of chemical fertilizers and the improper treatment of wastewater have led to several environmental problems such as increasing the concentration of nitrate in underground and surface water. A high concentration of nitrate in drinking water leads to the production of nitrosamine, which is related to cancer [1]. Nitrites react directly with hemoglobin in the blood of people to produce methemoglobin,

which destroys the ability of blood cells to transport oxygen [2]. Nitrates have also a negative effect on the aquatic plant growth, thus it has the same negative impact on the quality of water [3]. Because of all the previous serious ailments affects both wildlife and humans [4]. The Environmental Protection Agency (EPA) has since adopted the 10 mg/L standard as the maximum contaminant level (MCL) for nitrate-nitrogen and the 50 mg/L standard for nitrate [5].

Many methods are used to detect nitrates such as: distillation, reverse osmosis, ion exchange, and adsorption [6].

* Corresponding author.

Distillation is a very simple, rapid, and reliable technique for the termination of nitrate. However, the amount of energy required by the unit compared with the small volume of water produced limits the distillation to certain applications [7]. The reverse osmosis process has a drawback as the actual removal rates depend on the initial quality of the water, the system pressure, and the water temperature [8]. Another effective method used for nitrate removal is ion exchange by special anion exchange resins [9]. Ion exchange has a drawback as the resin prefers the sulfate exchange and water high in sulfates hinders the nitrate exchange that reduces the system effectiveness [10]. After comparing with these methods, adsorption has found to be superior to other techniques for water treatment in terms of initial cost, flexibility, simplicity of design, and ease of operation [11].

Chitosan is a biopolymer obtained by a full or partial N-deacetylation of chitin, which is known as a major component of the crustacean exoskeletons [12]. It has been proved to have desirable qualities, such as hemostasis, bacteriostasis, and biocompatibility [13]. Chitosan has been used in various applications such as the removal of metal ions, anions, and dyes [14–17]. It has many function groups such as hydroxyl and primary amine groups; hence, most of the chemical modifications are made with respect to these functional groups. It can be modified by chemical substituents that have functional groups such as carboxylic acid or thionyl groups which play an important role in the adsorption process [18].

Inorganic nano-materials are usually chosen to improve the stability of the polymeric phase and to introduce new chemical properties. Common choices of inorganic layers include silica, titania, zirconia, and other metal oxides. Cs along with metal oxide is an ideal bio-polymeric material because it has high biocompatibility, disintegration, non-toxicity, antibacterial, and hydrophilic properties [19].

The aim of this study is effective adsorption of nitrate ions from aqueous solutions by the usage of economical ecofriendly adsorbents. Cs/Gltn/PDMAEMA, Cs/Gltn/PDMAEMA-treated, and Cs/Gltn/PDMAEMA-SiO₂ composite were prepared for this purpose. The effects of contact time, dosage of sorbent, initial concentration, pH, and temperature on adsorption have been investigated. Adsorption kinetic and isotherm models were applied to analyze the kinetics and nature of adsorption. The thermodynamic parameters have been also evaluated.

2. Materials and methods

2.1. Materials

2-(N,N-Dimethylamino) ethyl methacrylate (DMAEMA) and silica (SiO₂) were supplied from (Sigma-Aldrich, USA). Chitosan (Cs) (85% DA) of medium molecular weight is supplied from Meron. The Gelatin was supplied from El-Nasr Pharmaceutical Chemical-Prolabo (Cairo, Egypt). Other chemicals were purchased from El-Nasr Co. (Cairo, Egypt). The chemical structures of chitosan, DMAEMA, and gelatin are shown in Fig. 1.

2.2. Preparation of Cs/Gltn/PDMAEMA hydrogel

A 1.5% Cs solution (w/v) was prepared by dissolving 1.5 g of Cs in 100 ml of deionized H₂O containing 1% (v/v) of

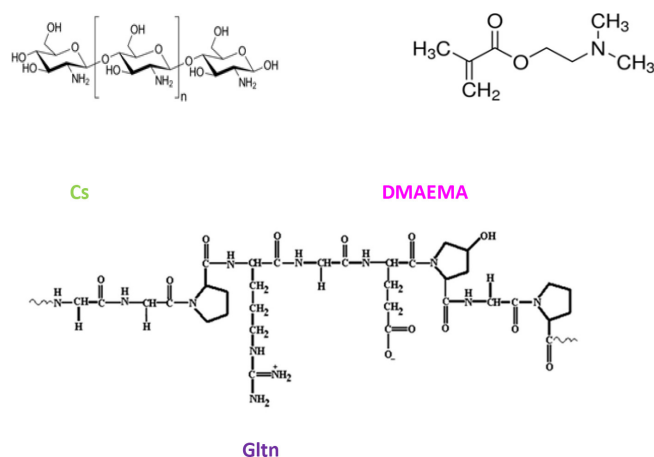


Fig. 1. The chemical structures of chitosan, DMAEMA, and gelatin.

acetic acid at 60°C in water bath with stirring for 1 h. A 20% of gelatin solution (w/v) was prepared by dissolving 20g of gelatin in 100 ml of deionized water at 60°C for 30 min in water bath. Subsequently, the two solutions were mixed in equal ratios. DMAEMA in a concentration of 0.36 (g/g) was added to the solution where its concentration in the mixture solution became 20 wt%. The mixture was irradiated at 15 kGy using ⁶⁰Co gamma source installed at the National Centre for Radiation Research and Technology (NCRRT), Egypt. The prepared hydrogel was extracted in distilled water at 80°C for 2 h to remove the non-cross linked polymer then it was air-dried.

2.3. Preparation of Cs/Gltn/PDMAEMA/SiO₂ composite

A 0.03 g of SiO₂ powder was added to a 100 ml of deionized H₂O containing 1% (v/v) acetic acid solution then sonicated for 30 min. After sonication, 1.5 g of the Cs was added and stirred for 1 h at 60°C in water bath. Consequently, the above steps for the preparation of Cs/Gltn/PDMAEMA hydrogel were followed.

2.4. Preparation of the treated Cs/Gltn/PDMAEMA hydrogel

A mixture of 15 g of Cs/Gltn/PDMAEMA hydrogel, 15 g thiourea, 50 ml HCl, and 150 ml H₂O were mixed in a one-neck flask and stirred for 24 h [20]. After that, the swelled hydrogel was washed and transferred to another flask containing 10% (w/v) NaOH and was stirred with a magnetic stirrer for another 6 h. After filtration, the hydrogel was washed with acetone, ethanol, and deionized water. Finally, it was dried at 50°C.

2.5. The swelling measurements

The clean, dried, weighed sample was soaked in bi-distilled water or buffer solution at room temperature in different time intervals. The sample was taken and the excess water on the surface was removed by blotting quickly with a filter paper then the sample was reweighed. The swelling percentage was calculated as follows:

$$\text{Swelling (\%)} = \frac{W_s - W_d}{W_d} \times 100 \quad (1)$$

where W_d and W_s are the masses of dry and swelled sample, respectively.

2.6. Adsorption procedure Study

Adsorption experiments were carried out by batch equilibration method in duplicate. Nitrate determination was carried out according to the complex formed by nitration of salicylic acid under highly acidic conditions. The complex absorbs maximally at 410 nm in basic medium (pH > 12). The absorbance of the chromophore is directly proportional to the concentration of NO_3^- present. Ammonium, nitrate, and chloride ions do not interfere.

The effect of contact time on the adsorption of NO_3^- was investigated in the period from 15 to 180 min using 20 mg/L of NO_3^- solution and 0.05 g of adsorbent at room temperature in a mechanical shaker having 120 rpm. The effect of initial concentration was studied by varying the concentrations of NO_3^- in the range of 20–100 mg/L. Dosage effect of the adsorbents was investigated by varying the dose between 0.05 and 0.3 g. The pH effect was investigated by adjusting the pH of NO_3^- solutions as 2, 4, 6, and 8 using 0.1 mol/L HCl and NaOH.

3. Results and discussion

Gelatin and chitosan in this study are used to prepare a biodegradable based hydrogel with DMAEMA monomer by the effect of gamma radiation. The hydrogel in aqueous solution proceed by free radical mechanism. The energy of gamma radiation is absorbed by all elements of the system, in which the solvent (water) usually absorbs most of the energy. DMAEMA monomer contains unsaturated C=C double bond which undergoes degradation under the effect of gamma irradiation. Radiolysis of water involves the formation of hydroxyl radicals, which attack the polymer chains thus leading to the macroradicals formation [21]. Both polymerization and crosslinking processes are proceeded as shown in Fig. 2.

Treatment of Cs/Gltn/PDMAAEMA hydrogel with thiourea was done as shown in Fig. 3. The purpose of this treatment is increasing the hydrophilicity of the polymeric network. This means that an increment in swelling capacity is produced when contact with water. Whatever, it permits diffusion of more pollutants present in the aqueous solutions.

Incorporation of silica in the polymeric matrix of Cs/Gltn/PDMAAEMA has also been done to obtain Cs/Gltn/PDMAAEMA/SiO₂ composite. The presence of inorganic particles may affect the adsorption extend towards NO_3^- ions. The reaction of chitosan with silica is shown in Fig. 4.

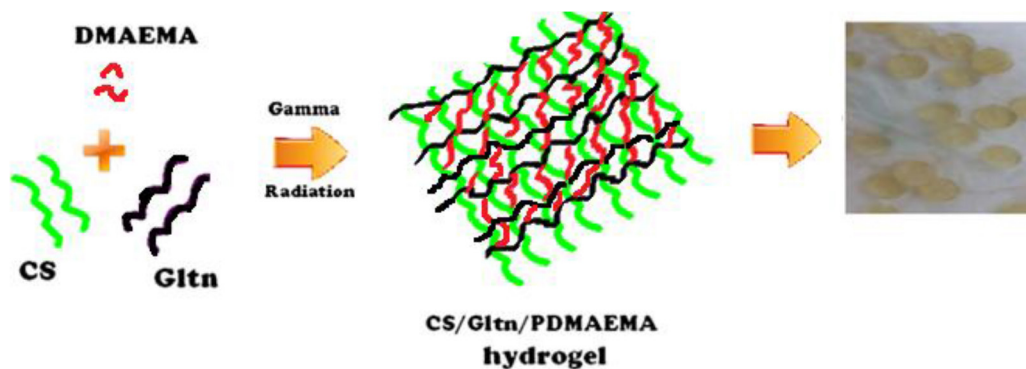


Fig. 2. Schematic illustration of the synthesis of Cs/Gltn/PDMAEMA hydrogel.

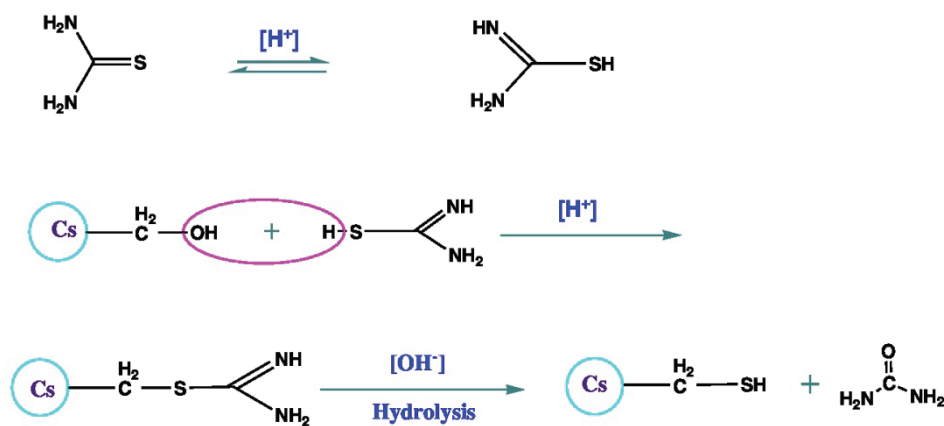


Fig. 3. The reaction mechanism of treatment of chitosan by thiourea.

The –OH groups in Cs get into the condensation reaction with silanol group of silica and resulted in the formation of Si–O–C bonds [22]. In addition, the amine groups of the polymeric matrix could form hydrogen bonds with silanol group of silica [23].

3.1. FTIR spectroscopy

The FTIR spectra of (Cs/Gltn/PDMAEMA) hydrogel, (Cs/Gltn/PDMAEMA)-treated, and Cs/Gltn/PDMAEMA/SiO₂ composite are shown in Fig. 5. The characteristic peaks of (Cs/Gltn/PDMAEMA) hydrogel were shown at 3,265 cm⁻¹ are corresponding to O–H stretching peak and overlapped with N–H stretching peak. The peaks at 2,941 and 2,828 cm⁻¹ are corresponding to the asymmetric and symmetric stretching peak of CH₂ groups in a saccharide

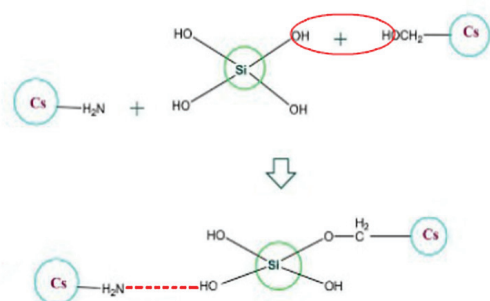


Fig. 4. Schematic representation of the interaction between chitosan and silica

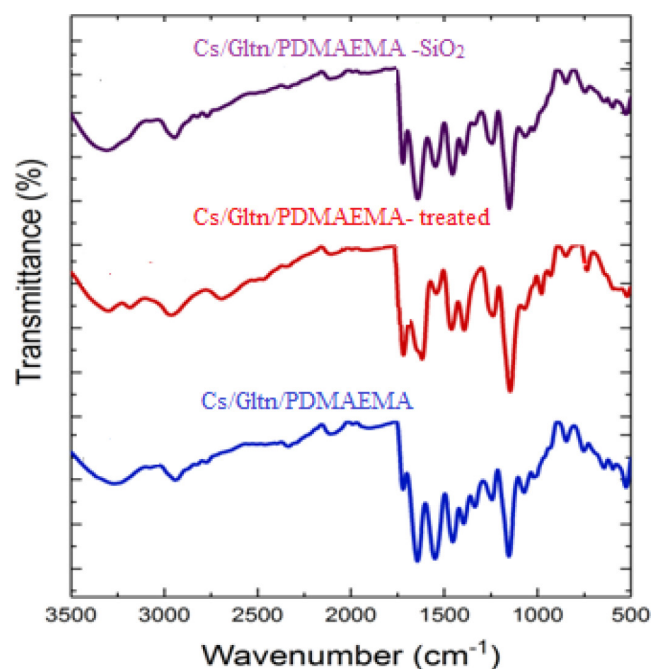


Fig. 5. FTIR spectra of Cs/Gltn/PDMAEMA, Cs/Gltn/PDMAEMA-treated and Cs/Gltn/PDMAEMA-SiO₂ composite.

ring, respectively [24]. The peaks at 1,454 and 1,336 cm⁻¹ are corresponding to CH₂ bending vibration. The peak at 1,153 cm⁻¹ is corresponding to C–O–C stretching in glycosidic bonds. The peaks at 1,072 and 1,020 cm⁻¹ are corresponding to the stretching peaks of secondary and primary C–O [25]. The peaks at 1,550 and 1,643 cm⁻¹ are corresponding to the stretching carbonyl group of amino group in Gltn. The 1,720 and 1,244 cm⁻¹ are corresponding to the ester and tertiary amino groups in DMAEMA, respectively. Comparing the FT-IR spectrum of (Cs/Gltn/PDMAEMA) hydrogel with the treated one, it can be observed that a new peak is observed at 2,513 cm⁻¹ which belongs to the–SH stretch. It showed that the thiol group was successfully introduced. Moreover, the peak at 1,020 cm⁻¹ associated with the primary hydroxyl group in the spectrum of (Cs/Gltn/PDMAEMA) hydrogel disappeared, whilst the peak at 1,072 cm⁻¹ of the secondary hydroxyl group did not change. The disappearance of the peak associated with the primary hydroxyl group could be due to the change of OH groups of C6–OH into SH groups which indicates that the thiolation occurred at the C6–OH of the chitosan [25]. In the spectrum of Cs/Gltn/PDMAEMA/SiO₂ composite, peaks are seen in the range of 963–846 cm⁻¹ are the typical peaks of Si–OH vibration.

3.2. Swelling studies

Fig. 6 shows the swelling percentage as a function of time of Cs/Gltn/PDMAEMA, Cs/Gltn/PDMAEMA-treated, and Cs/Gltn/PDMAEMA-SiO₂ composite at pH 7. It can be observed that a higher swelling ratio was obtained for all investigated systems. All systems showed a rapid increase in water content with increasing time and they reached equilibrium state in approximately 140 min. The presence of hydrophilic groups in the networks; COOH, –OH, and –NH₂ are responsible for the higher swelling percentage. Cs/Gltn/PDMAEMA/SiO₂ composite revealed the highest swelling percentage followed by Cs/Gltn/PDMAEMA-treated then Cs/Gltn/PDMAEMA hydrogels. The highest swelling ratio of the composite can be explained by the presence of silanol groups, which make the surface is highly hydrophilic [26]. For Cs/Gltn/PDMAEMA-treated, the treatment of Cs with thiourea enhanced the number of mobile ions inside the network structure due to the formation of S⁻ and H₃O⁺ ions [Eq. (2)]. This lead to a higher osmotic pressure inside the hydrogel network [23]. Therefore, the treated hydrogel has a higher swelling percentage compared to the untreated one.



The effect of pH on the swelling behavior of Cs/Gltn/PDMAEMA, Cs/Gltn/PDMAEMA-treated, and Cs/Gltn/PDMAEMA-SiO₂ composite is summarized in Fig. 7. It can be seen that the swelling percentage decreased with increasing pH value for all investigated systems. This means Cs/Gltn/PDMAEMA, Cs/Gltn/PDMAEMA-treated and Cs/Gltn/PDMAEMA-SiO₂ composite swelled better in acidic medium. The high swelling percentage at low pH values resulted from the protonation of –NH₂–NH(CH₂)₂–, –(SH),

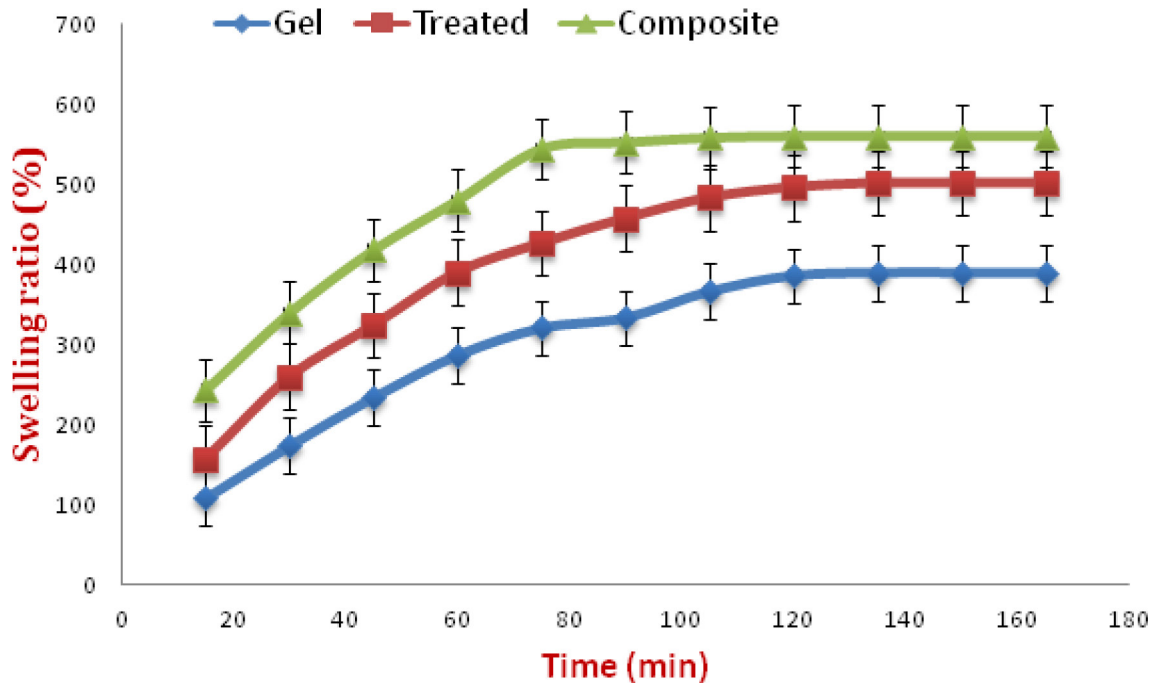


Fig. 6. Swelling kinetics of Cs/Gln/PDMAEMA, Cs/Gln/PDMAEMA-treated and Cs/Gln/PDMAEMA-SiO₂ composite at 25°C and pH 7.

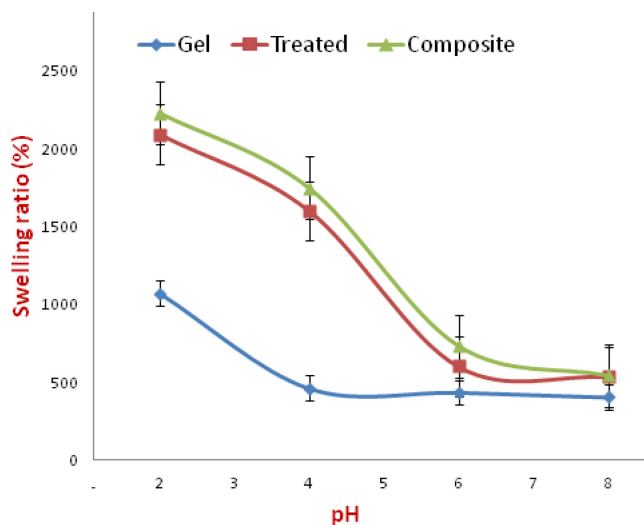


Fig. 7. Equilibrium swelling percent of Cs/Gln/PDMAEMA, Cs/Gln/PDMAEMA-treated and Cs/Gln/PDMAEMA-SiO₂ composite as a function of pH at time; 24 h, and 25°C.

and $\equiv\text{Si}-\text{OH}$ forming $-\text{NH}_3^+$, $\text{NH}_2^+(\text{CH}_3)_2$, SH_2^+ , and $\equiv\text{Si}-\text{OH}_2^+$, respectively. The protonation led to a repulsion between the polymer chains allowing more water to be absorbed into the network. At higher pH values, deprotonation of these groups occurred, repulsion of polymer chains receded and hence the swelling decreased. The surface charge of Cs is positive in acidic pH, it gradually decreased with increasing the pH and it has zero potential at pH 6.4 [27]. On the other hand, at higher pH values, deprotonation of the carboxylic group in Gln occurred and a repulsion of the negatively charged polymer chains resulted from COO^- groups occurred [28].

However, the swelling percentage decreased at high pH values which indicates that cationic gels tended to swell higher than the anionic ones [29].

3.3. Adsorption study

3.3.1. Effect of contact time

Effect of contact time on the adsorption of nitrate ions by Cs/Gln/PDMAEMA, Cs/Gln/PDMAEMA-treated, and Cs/Gln/PDMAEMA/SiO₂ composite was investigated as shown in Fig. 8. It can be observed that the adsorption capacity towards NO_3^- ions increased with increasing the contact time for all systems until it reached equilibrium within approximately 100 min. It can be noted that the adsorption rate was initially fast and the rate slowed down with time until equilibrium. The initial fast adsorption rate is probably due to the high availability of active sites on the surface of the adsorbent. Moreover, the attractive forces between NO_3^- and adsorbent surface such as Vander Waals forces and electrostatic attractions increased the diffusion into the matrix until reaching equilibrium [30]. Cs/Gln/PDMAEMA/SiO₂ composite revealed the highest values of adsorption capacity followed by Cs/Gln/PDMAEMA-treated then Cs/Gln/PDMAEMA hydrogel. The reason is that the higher number of functional groups and active sites increased the adsorption capacity and removal percentage as explained in Fig. 9.

3.3.2. Effect of pH

The effect of pH on the adsorption of NO_3^- ions is shown in Fig. 10. As seen in the figure, the highest value of adsorption capacity and removal was achieved at pH 2 for all investigated systems. The adsorption increased with decreasing pH of the

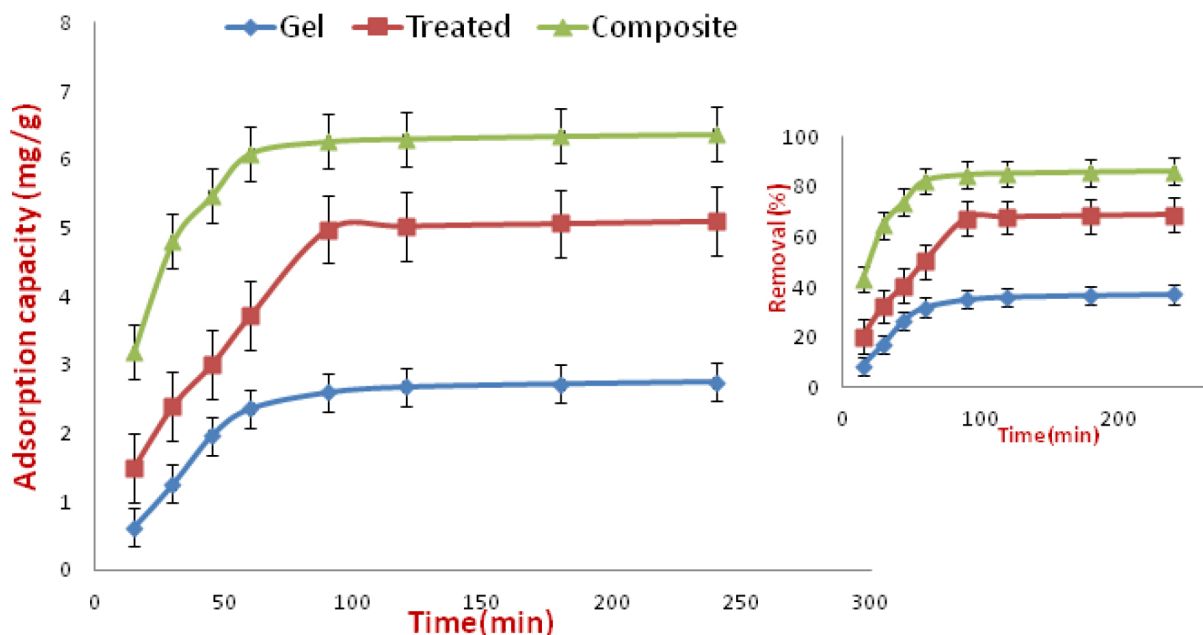
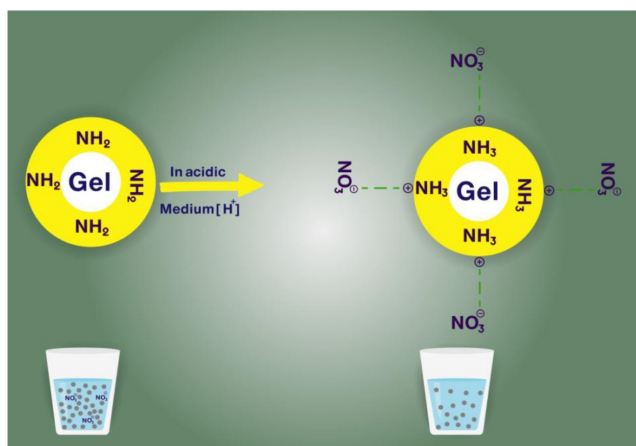


Fig. 8. Effect of time on the adsorption of NO_3^- by Cs/GltN/PDMAEMA, Cs/GltN/PDMAEMA-treated and Cs/GltN/PDMAEMA - SiO_2 composite at ambient temperature, pH 2, initial concentration; 18.5 mg/L and adsorbent dose; 2.5 g/L.



solution. At low pH values, more protons are available for protonation ($-\text{NH}_2$, $-\text{NH}(\text{CH}_3)_2$, SH , and $\equiv\text{Si}-\text{OH}$) and they generate positive sites such as ($-\text{NH}_3^+$, $-\text{NH}_2^+(\text{CH}_3)_2$, $-\text{SH}_2^+$ and $\equiv\text{Si}-\text{OH}_2^+$). This resulted in an enhancement of NO_3^- ions adsorption due to increasing the electrostatic interactions between positively charged sites and negatively charged nitrate groups. The nitrate adsorption capacity significantly decreased at basic pH values because at higher pH values the surface of the adsorbents acquires more negatively charge which repels NO_3^- ions and hence a reduction in adsorption was observed.

3.3.3. Effect of initial concentration

Fig. 11 shows the effect of initial NO_3^- ions concentration on the adsorption of Cs/GltN/PDMAEMA, Cs/GltN/PDMAEMA-treated and Cs/GltN/PDMAEMA/ SiO_2 composite. The sorption capacity for of NO_3^- ions significantly increased with increasing NO_3^- ions concentration. It is well-known that the more concentrated the solution, the better the adsorption due to the increase in adsorbate ions, which increases the interaction probability with the adsorbent surface. On the other hand, the removal percentage decreased by increasing NO_3^- ions concentration. This may be because at higher adsorbate concentration, the binding capacity of the adsorbent approaches saturation resulting in a decrease in overall removal percentage [31].

3.3.4. Effects of temperature

The sorption of nitrates from their aqueous solutions by Cs/GltN/PDMAEMA, Cs/GltN/PDMAEMA-treated, and Cs/GltN/PDMAEMA/ SiO_2 composite at different temperatures is shown in Fig. 12. It can also be observed that the equilibrium adsorption capacity decreased by increasing the temperature

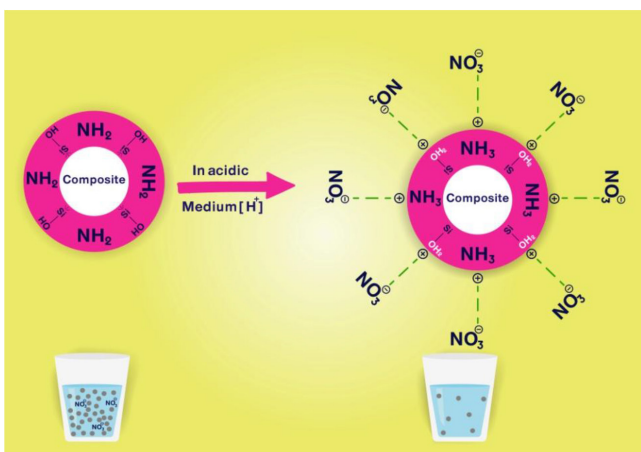


Fig. 9. A diagram presents the adsorption of NO_3^- by Cs/GltN/PDMAEMA hydrogel and Cs/GltN/PDMAEMA- SiO_2 composite.

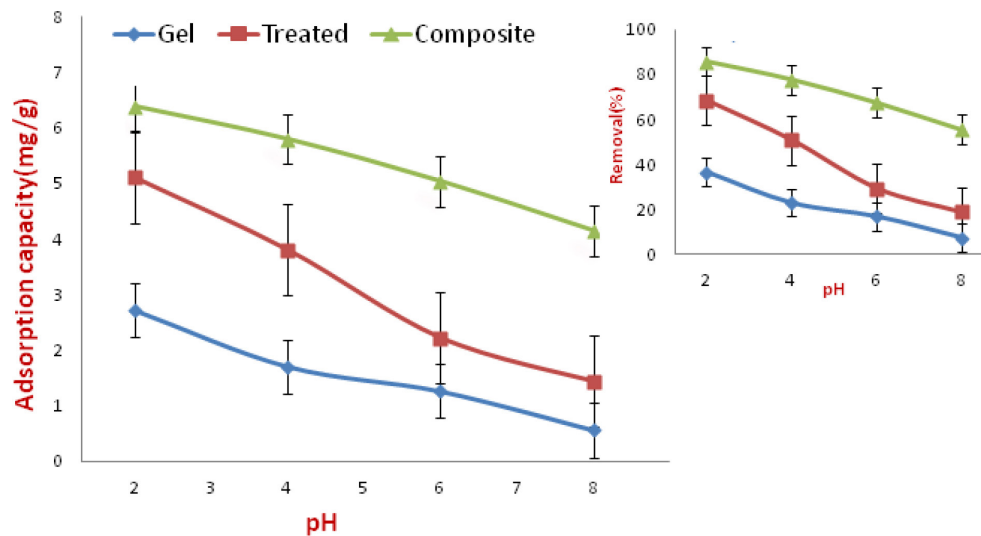


Fig. 10. Effect of pH on the adsorption of NO_3^- by Cs/Gln/PDMAEMA, Cs/Gln/PDMAEMA-treated and Cs/Gln/PDMAEMA - SiO_2 composite at ambient temperature, time; 240 min, initial concentration 18.5 mg/L, and adsorbent dose; 2.5 g/L.

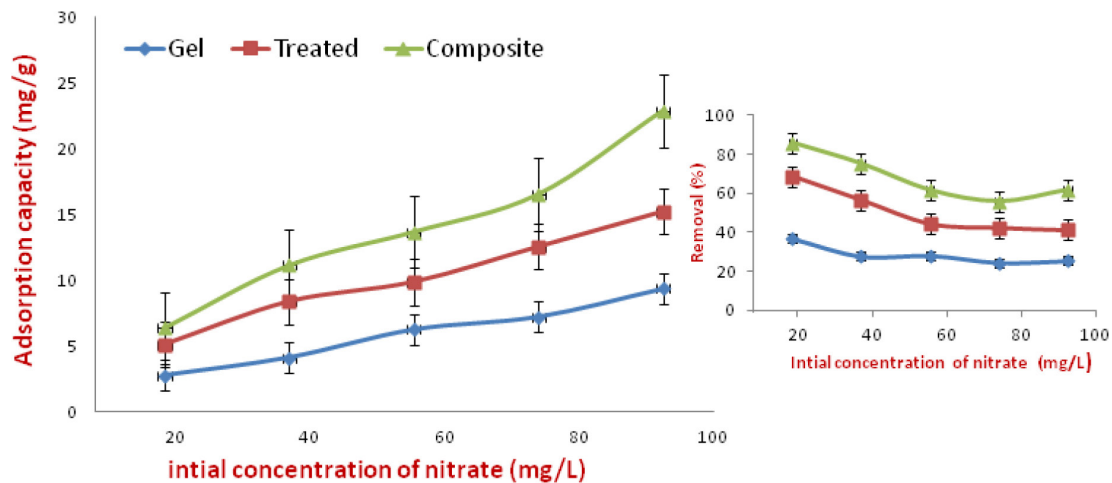


Fig. 11. Effect of initial concentration on the adsorption of NO_3^- by Cs/Gln/PDMAEMA, Cs/Gln/PDMAEMA-treated and Cs/Gln/PDMAEMA - SiO_2 composite at ambient temperature, time; 240 min, pH 2, and adsorbent dose; 2.5 g/L.

from 30°C to 60°C, the maximum sorption of nitrate ions was at 30°C. A decrease in the uptake values with rising temperature may be due to the damage of active binding sites of the adsorbent or due to increasing tendency to desorb ions from the interface to the solution. This result indicates the exothermic nature of these adsorption processes onto the surface of all investigated systems.

3.3.5. Effect of adsorbent dose

Fig. 13 shows the effect of adsorbent dosage on the adsorption capacity of NO_3^- ions onto Cs/Gln/PDMAEMA, Cs/Gln/PDMAEMA-treated, and Cs/Gln/PDMAEMA/ SiO_2 composite. The adsorption capacity decreased as the adsorbent dosage increased because the adsorptive capacity of adsorbent available was not fully utilized at a higher adsorbent dosage in comparison to lower adsorbent dosage [32]. On the other hand, the removal percentage of NO_3^- ions increased as the sorbent dosage increased.

The reason was that the number of active site available for adsorption increased, leading to an increase in the removal percentage [33]. A little increase in adsorption was obtained by increasing the sorbent dosage from 0.2 to 0.3 g/20 mL. This means that from the economical point of view, the optimum sorbent dosage is 0.2 g/20 mL (10 g/L).

3.4. Adsorption kinetics

In order to study the controlling mechanisms of the adsorption process, pseudo-first-order [32] and pseudo-second-order [33] kinetic models are used to fit the experimental kinetic data.

The linear form of the pseudo-first order model is explained as the following:

$$\log(q_e - q_t) = \log q_e - \frac{k_1}{2.303} t \quad (3)$$

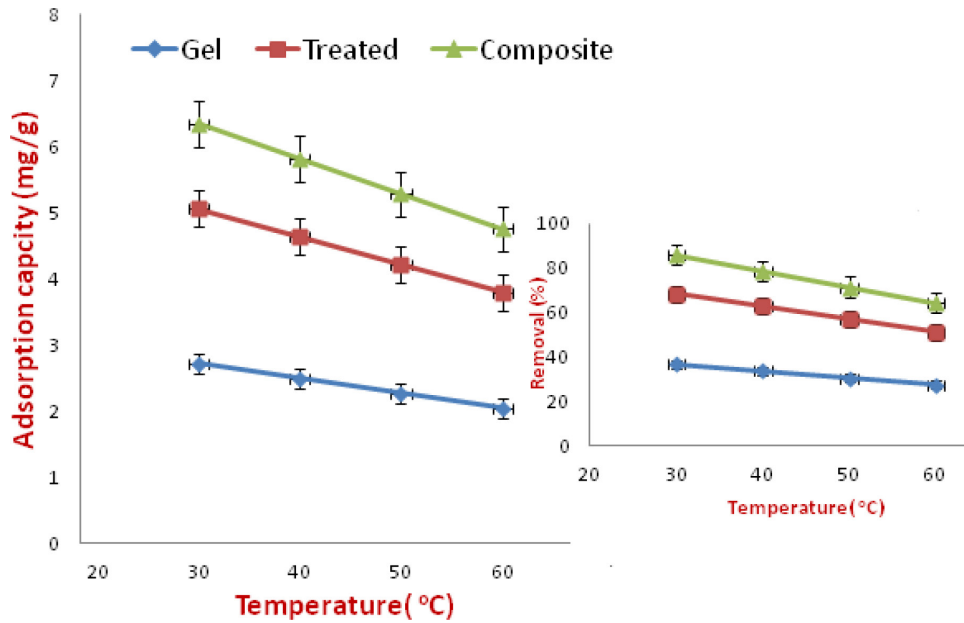


Fig. 12. Effect of temperature on the adsorption of NO_3^- by Cs/Gln/PDMAEMA, Cs/Gln/PDMAEMA-treated and Cs/Gln/PDMAEMA-SiO₂ composite at time; 240 min, initial concentration; 18.5 mg/L, pH 2, adsorbent dose; 2.5 g/L.

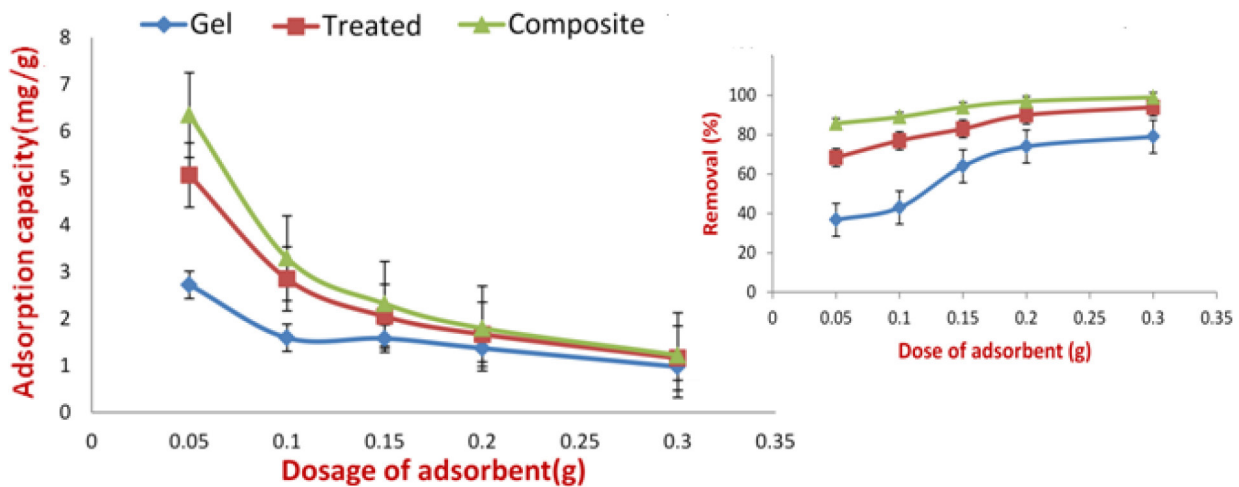


Fig. 13. Effect of adsorbent dose on the adsorption of NO_3^- by Cs/Gln/PDMAEMA, Cs/Gln/PDMAEMA-treated and Cs/Gln/PDMAEMA-SiO₂ composite at ambient temperature, time; 240 min, pH 2, and initial concentration 18.5 mg/L

where q_e and q_t are the sorption capacity at equilibrium and at time t , respectively (mg/g). k_1 (1/min) is the rate constant of pseudo first-order adsorption.

The pseudo second order kinetic model is represented by the following linear equation:

$$\frac{t}{q_t} = \frac{1}{k_2 q_e^2} + \frac{1}{q_e} t \tag{4}$$

where k_2 (1/min) is the rate constant of pseudo second order sorption.

Upon correlation of the kinetic data of the investigated systems with the above two rate models, by plotting $\log(q_e - q_t)$ vs. t for pseudo-first order model [Eq. (2)]

and plotting t/q_t against t of pseudo second order kinetic model [Eq. (3)] as shown in Fig. 14. The obtained data for pseudo-first-order and pseudo-second-order models is shown in Table 1. It can be observed that the correlation coefficients (R^2) of pseudo-second-order are higher than that of pseudo-first-order model. These indicated that the adsorption of NO_3^- ions by Cs/Gln/PDMAEMA, Cs/Gln/PDMAEMA-treated, and Cs/Gln/PDMAEMA/SiO₂ composite is described well using pseudo-second-order model.

3.5. Adsorption isotherms

The adsorption isotherm is fundamental in demonstrating the nature of the interaction between adsorbate and adsorbent. In this investigation, the equilibrium adsorption data

were analyzed using the Langmuir [34] and the Freundlich [35] isotherm models

$$\frac{C_e}{q_e} = \frac{C_e}{Q} + \frac{1}{Qb} \quad (5)$$

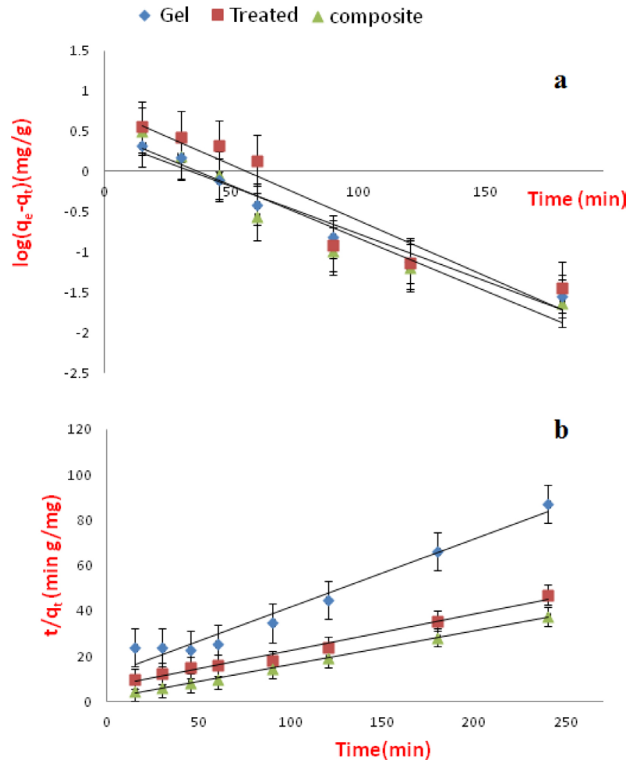


Fig. 14. Pseudo first order (a) and Pseudo second order (b) kinetic plots for adsorption of NO_3^- by Cs/Gltn/PDMAEMA, Cs/Gltn/PDMAEMA-treated and Cs/Gltn/PDMAEMA- SiO_2 composite.

$$\ln q_e = \ln Q_F + \frac{1}{n} \ln C_e \quad (6)$$

where C_e (mg/L) is the equilibrium NO_3^- concentration in the solution, q_e (mg/g) is the NO_3^- concentration in the adsorbent, b is the Langmuir constant (L/mg) that relates to the affinity of binding sites and Q is the theoretical saturation capacity of the monolayer (mg/g). Q_F (L/g) is the Freundlich constant, and $1/n$ is the heterogeneity factor.

The Langmuir isotherm model [Eq. (4)] assumes that the intermolecular forces decrease rapidly with distance. This leads to a monolayer coverage of the adsorbate at specific homogeneous sites on the outer surface of the adsorbent (chemical adsorption). Whereas the Freundlich model [Eq. (5)] assumes that, the sorbent surface is heterogeneous in nature with an exponential distribution of active sites where an unlimited number of sorption sites are available.

The two isotherm models were applied to the investigated systems (Fig. 15) and the isotherm model parameters were evaluated as shown in Table 2. It can be observed from the values of the correlation coefficient (R^2) that the Freundlich model provided a better linearity than the Langmuir model. The predicted equilibrium adsorption values using Langmuir isotherm do not fit with experimental equilibrium adsorption data. This means that the adsorption is not characterized by chemical nature. The relatively high values of the correlation coefficients (R^2) obtained from the Freundlich isotherm model indicated that the

Table 1

Pseudo-first-order and pseudo-second-order kinetic parameters for adsorption of NO_3^- ions by Cs/Gltn/PDMAEMA, Cs/Gltn/PDMAEMA-treated and Cs/Gltn/PDMAEMA/ SiO_2 composite

Item	Cs/Gltn/PDMAEMA	Cs/Gltn/PDMAEMA-treated	Cs/Gltn/PDMAEMA/ SiO_2
Pseudo-first-order model			
R^2	0.9241	0.9024	0.9241
$k_1 \times 10^{-2}$ (min^{-1})	2.7175	3.2011	3.0169
$q_{e, \text{cal}}$ (mg/g)	2.5760	5.9530	2.9970
Pseudo-second-order model			
R^2	0.9678	0.9825	0.998
$k_2 \times 10^{-3}$ (min^{-1})	7.4289	3.9997	14.0308
$q_{e, \text{cal}}$ (mg/g)	3.3500	6.1919	6.7340
$q_{e, \text{exp}}$ (mg/g)	2.7	5.1	6.37
Column1	Gel	Treated	Composite
R^2	0.9651	0.9024	0.9241
Intercept: $\log q_e$	0.4111	0.7748	0.4767
Slope: $K1/2.303$	-0.0118	-0.0139	-0.0131
K1	-0.0271754	-0.0320117	-0.0301693
Calculated q_e	2.576	5.953	2.997
Experimental q_e	2.7	5.1	6.37

adsorption process is heterogeneous. This means that the adsorption process mainly physical adsorption that may occur by electrostatic interaction of the opposite charge. On the other hand, the heterogeneity factor of $1/n$ is a measure of the favorability of adsorption and the degree of heterogeneity of adsorbate at the adsorbent surface. $1/n$ is less than unity what indicates a favorable adsorption. The more heterogeneous the surface, the closer $1/n$ value is to 0 [35]. This indicates that the NO_3^- is favorably adsorbed onto Cs/Gltn/PDMAEMA, Cs/Gltn/PDMAEMA-treated and Cs/Gltn/PDMAEMA/SiO₂ composite. The favorability of adsorption is ordered according to the value of $1/n$ in sequence of Cs/Gltn/PDMAEMA/SiO₂ > Cs/Gltn/PDMAEMA-treated > Cs/Gltn/PDMAEMA.

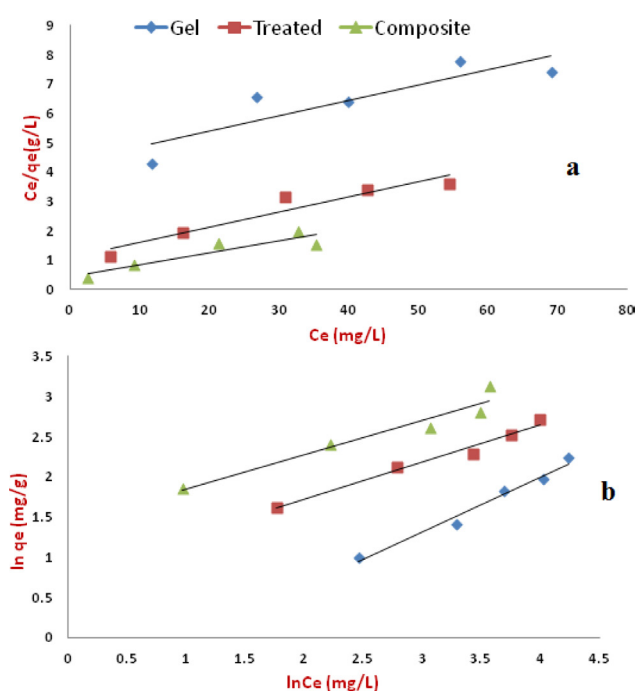


Fig. 15. Langmuir (a) and Freundlich (b) isotherm models plots for adsorption of NO_3^- by Cs/Gltn/PDMAEMA, Cs/Gltn/PDMAEMA-treated and Cs/Gltn/PDMAEMA-SiO₂ composite.

Table 2

Langmuir and Freundlich isotherm constants for adsorption of NO_3^- ions by Cs/Gltn/PDMAEMA, Cs/Gltn/PDMAEMA-treated and Cs/Gltn/PDMAEMA/SiO₂ composite

Item	Cs/Gltn/PDMAEMA	Cs/Gltn/PDMAEMA-treated	Cs/Gltn/PDMAEMA/SiO ₂
Langmuir isotherm model			
R^2	0.7735	0.9145	0.8511
Q (mg/g)	19.1204	3.9401	24.5098
b (L/mg)	0.0119	4.0608	0.0922
Freundlich isotherm model			
R^2	0.9756	0.9764	0.9338
$1/n$	0.6848	0.464	0.4256
n	1.4602	2.1551	2.3496
Q_f	2.0861	2.2122	4.1682

3.6. Thermodynamic study

The thermodynamic parameters; enthalpy change (ΔH°) and entropy change (ΔS°) of NO_3^- adsorption onto Cs/Gltn/PDMAEMA, Cs/Gltn/PDMAEMA-treated and Cs/Gltn/PDMAEMA/SiO₂ composite can be evaluated by the van't Hoff [36].

$$\ln k = \frac{\Delta S^\circ}{R} - \frac{\Delta H^\circ}{RT} \quad (7)$$

where $k = \text{Fe}/(1-\text{Fe})$, and $\text{Fe} = (C_o - C_e)/C_o$, T is the temperature in a degree of K and R is the gas constant (8.314 J/mol K). ΔH° and ΔS° have been obtained from the slope and the intercept of the plot of $\ln k$ vs. $1/T$ (Fig. 16) and the analyzed data is summarized in Table 3. It was obtained that the values of ΔH° are negative for all investigated systems and they are lower than 40 kJ/mol which indicates exothermic physisorption nature of adsorption. Therefore, the adsorption processes were not favorable at higher temperatures. Moreover, the affinity of NO_3^- for adsorption onto Cs/Gltn/PDMAEMA, Cs/Gltn/PDMAEMA-treated and Cs/Gltn/PDMAEMA/SiO₂ composite may be due to Van der Waals forces and electrostatic attractions between NO_3^- and the positively sites on the surface of the adsorbent. The negative values of ΔS° refracted a random decrease at the solid/liquid interface during the adsorption.

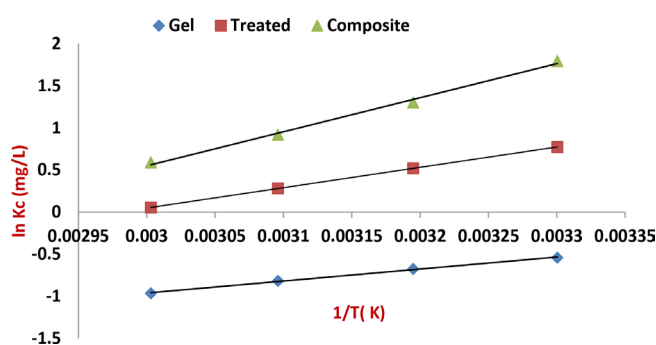


Fig. 16. van't Hoff model plot for adsorption of NO_3^- by Cs/Gltn/PDMAEMA, Cs/Gltn/PDMAEMA-treated and Cs/Gltn/PDMAEMA-SiO₂ composite.

Table 3

Thermodynamic parameters for adsorption of NO_3^- ions by Cs/Gln/PDMAEMA, Cs/Gln/PDMAEMA-treated and Cs/Gln/PDMAEMA/SiO₂ composite

Item	Cs/Gln/PDMAEMA	Cs/Gln/PDMAEMA-treated	Cs/Gln/PDMAEMA/SiO ₂
R ²	0.997	0.999	0.996
ΔH° (KJ/mol)	-11.82	-20.13	-33.65
ΔS° (J/mol K)	-43.45	-59.99	-96.37
ΔG°_{303} (KJ/mol)	3,140.75	4,244.58	5,726.22
ΔG°_{313} (KJ/mol)	3,173.90	4,094.34	5,106.20
ΔG°_{323} (KJ/mol)	3,206.80	3,977.28	4,712.68
ΔG°_{333} (KJ/mol)	3,239.38	3,883.82	4,436.26

The values of the standard Gibbs free energy change (ΔG°) were estimated using the following equation:

$$\Delta G^\circ = \Delta H^\circ - T\Delta S^\circ \quad (8)$$

As seen in Table 3, (ΔG°) values at all studied temperatures were positive which indicated that these adsorption processes are not spontaneous in nature and the adsorption reaction requires energy from outside of the system. The increase in the ΔG° value with increasing temperature for Cs/Gln/PDMAEMA hydrogel indicated that the adsorption process becomes less favorable at high temperatures. In case of Cs/Gln/PDMAEMA-treated and Cs/Gln/PDMAEMA/SiO₂ composite, (ΔG°) decreased with increasing temperature indicating that the adsorption process is favorable at higher temperatures, however, the low adsorption at higher temperatures may be due to the increase of the kinetic energy.

4. Conclusion

(Cs/Gln/PDMAEMA) hydrogel was prepared by gamma irradiation and was modified with thiourea to convert the hydroxyl groups into thiol groups. Also, incorporation of SiO₂ in the hydrogel was done to form Cs/Gln/PDMAEMA/SiO₂ composite. Prepared hydrogels and the composite were used as adsorbent materials for removal of NO_3^- ions from aqueous solutions. The adsorbent parameters were studied for optimal conditions. It was found that the maximum adsorption was obtained at pH 2 within 100 min and the optimum sorbent dosage was 10 g/L. The removal percentage decreased with increasing of NO_3^- ions concentration. The adsorption kinetics was explained by a pseudo second-order equation with a good correlation. The adsorption isotherm was well-fitted to the Freundlich model. This means that the adsorption process is mainly a physical adsorption that may occur by electrostatic interaction of the opposite charge. The negative values of ΔH° for all investigated systems indicates the exothermic physisorption nature of adsorption. The negative values of ΔS° refracted a decrease in randomness at the solid/liquid interface during the adsorption.

References

- [1] M.F. Abou Taleb, G.A. Mahmoud, S.M. Elsigeny, E.-S.A. Hegazy, Adsorption and desorption of phosphate and nitrate ions using quaternary (polypropylene-g-N,N-dimethylamino ethylmethacrylate) graft copolymer, *J. Hazard. Mater.*, 159 (2008) 372–379.
- [2] M. Parvizishad, A. Dalvand, A.H. Mahvi, F. Goodarzi, A review of adverse effects and benefits of nitrate and nitrite in drinking water and food on human health, *Health Scope*, In Press (2017).
- [3] J.A. Baker, G. Gilron, B.A. Chalmers, J.R. Elphick, Evaluation of the effect of water type on the toxicity of nitrate to aquatic organisms, *Chemosphere*, 168 (2017) 435–440.
- [4] J.A. Camargo, A. Alonso, A. Salamanca, Nitrate toxicity to aquatic animals: a review with new data for freshwater invertebrates, *Chemosphere*, 58 (2005) 1255–1267.
- [5] B.E. Klein, J.A. McElroy, R. Klein, K.P. Howard, K.E. Lee, Nitrate-nitrogen levels in rural drinking water: is there an association with age-related macular degeneration, *J. Environ. Sci. Health A. Toxic Hazard. Subst. Environ. Eng.*, 48 (2013) 1757–1763.
- [6] W.J. Hunter, Chapter 17 - Remediation of Drinking Water for Rural Populations, in: R.F. Follett, J.L. Hatfield, Eds., *Nitrogen in the Environment: Sources, Problems and Management*, Elsevier Science, Amsterdam, 2001, pp. 433–453.
- [7] M. Akhtar, F. Hussain, T.M. Qureshi, M.Y. Ashraf, J. Akhter, A. Haq, Rapid and inexpensive steam distillation method for routine analysis of inorganic nitrogen in alkaline calcareous soils, *Commun. Soil Sci. Plant Anal.*, 42 (2011) 920–931.
- [8] J.J. Schoeman, A. Steyn, Nitrate removal with reverse osmosis in a rural area in South Africa, *Desalination*, 155 (2003) 15–26.
- [9] J. Kim, M.M. Benjamin, Modeling a novel ion exchange process for arsenic and nitrate removal, *Water Res.*, 38 (2004) 2053–2062.
- [10] S. Samatya, N. Kabay, Ü. Yüksel, M. Arda, M. Yüksel, Removal of nitrate from aqueous solution by nitrate selective ion exchange resins, *React. Funct. Polym.*, 66 (2006) 1206–1214.
- [11] A. Sowmya, S. Meenakshi, Effective removal of nitrate and phosphate anions from aqueous solutions using functionalised chitosan beads, *Desal. Wat. Treat.*, 52 (2014) 2583–2593.
- [12] D.E. Hegazy, G.A. Mahmoud, Radiation synthesis and characterization of polyethylene oxide/ chitosan-silver nanocomposite for biomedical application, *Arab J. Nucl. Sci. Appl.*, 47 (2014) 1–14.
- [13] M.A. Abdel Khalek, G.A. Mahmoud, N.A. El-Kelesh, Synthesis and characterization of poly-methacrylic acid grafted chitosan-bentonite composite and its application for heavy metals recovery, *Chem. Mater. Res.*, 2 (2012) 1–12.
- [14] C. Gerente, V.K.C. Lee, P. Le Cloirec, G. McKay, Application of chitosan for the removal of metals from wastewaters by adsorption—mechanisms and models review, *Crit. Rev. Environ. Sci. Technol.*, 37 (2007) 41–127.
- [15] F.W. Mahatmanti, W.D.P. Rengga, E. Kusumastuti, Nuryono, Adsorption of Pb(II) ion from aqueous solution onto chitosan/silica/polyethylene glycol (Ch/Si/P) composites membrane, *IOP Conference Series: Materials Science and Engineering* (2017), 172 (11th Joint Conference on Chemistry in conjunction with the 4th Regional Biomaterials Scientific Meeting, 2016), 012019/1-012019/6.
- [16] R. Joris, V.R. Stijn, B.C. Rao, V.G. Tom, M. Steven, B. Koen, Recovery of scandium from leachates of Greek bauxite residue

- by adsorption on functionalized chitosan silica hybrid materials, *Green Chem.*, 18 (2016) 2005–2013.
- [17] M. Aden, R.N. Ubol, M. Knorr, J. Husson, M. Euvrard, Efficient removal of nickel(II) salts from aqueous solution using carboxymethylchitosan-coated silica particles as adsorbent, *Carbohydr. Polym.*, 173 (2017) 372–382.
- [18] N.A. Mohamed, A. El-Ghany, Swelling behavior of cross-linked terephthaloyl thiourea carboxymethyl chitosan hydrogels, *Cell. Chem. Technol.*, 50 (2016) 463–471.
- [19] D. Sunil, Recent Advances on Chitosan-Metal Oxide Nanoparticles and Their Biological Application, in: *Materials Science Forum*, Trans Tech Publications, 2013, pp. 99–108.
- [20] B. Liua, X. Peng, W. Chen, Y. Li, X. Meng, D. Wang, G. Yub, Adsorptive removal of patulin from aqueous solution using thiourea modified chitosan resin, *Int. J. Biol. Macromol.*, 80 (2015) 520–528.
- [21] S.E. Abdel-Aal, G.A. Mahmoud, A.A. Elbayaa, N.A. Badway, D.F. Ahmed, Consecutive removal of hazardous dyes from aqueous solutions by composite hydrogels based on rice straw, *J. Res. Updates Polym. Sci.*, 6 (2017) 102–117.
- [22] T.M. Budnyak, I.V. Pylypchuk, V.A. Tertykh, E.S. Yanovska, D. Kolodynska, Synthesis and adsorption properties of chitosan-silica nanocomposite prepared by sol-gel method, *Nanoscale Res. Lett.*, 10 (2015) 1–10.
- [23] L.T.K. Dung, N.Q. Hien, D. Van Phu, B.D. Du, Effect of nanosilica/chitosan hybrid on leaf blast and blight diseases of rice in Vietnam, *Vietnam J. Chem.*, 54 (2016) 719–723.
- [24] Z. Modrzejewska, M. Dorabialska, R. Zarzycki, A. Wojtasz-Pajak, The mechanism of sorption of Ag⁺ ions on chitosan microgranules: IR and NMR studies, *Prog. Chem. Appl. Chitin Deriv.*, 14 (2009) 49–64.
- [25] A. Tiwari, L. Hihara, Thermal stability and thermokinetics studies on silicone ceramer coatings: part 1-inert atmosphere parameters, *Polym. Degrad. Stab.*, 94 (2009) 1754–1771.
- [26] L.T. Zhuravlev, The surface chemistry of amorphous silica. Zhuravlev model, *Colloids Surf. A.*, 173 (2000) 1–38.
- [27] S. Chatterjee, S.H. Woo, The removal of nitrate from aqueous solutions by chitosan hydrogel beads, *J. Hazard. Mater.*, 164 (2009) 1012–1018.
- [28] L. Cui, J. Jia, Y. Guo, Y. Liu, P. Zhu, Preparation and characterization of IPN hydrogels composed of chitosan and gelatin cross-linked by genipin, *Carbohydr. Polym.*, 99 (2014) 31–38.
- [29] A. Duconseille, T. Astruc, N. Quintana, F. Meersman, V. Sante-Lhoutellier, Gelatin structure and composition linked to hard capsule dissolution: a review, *Food Hydrocolloids*, 43 (2015) 360–376.
- [30] M.A. El-Latif, A.M. Ibrahim, M. El-Kady, Adsorption equilibrium, kinetics and thermodynamics of methylene blue from aqueous solutions using biopolymer oak sawdust composite, *J. Am. Sci.*, 6 (2010) 267–283.
- [31] G.A. Mahmoud, S.F. Mohamed, H.M. Hassan, Removal of methylene blue dye using biodegradable hydrogel and reusing in a secondary adsorption process, *Desal. Wat. Treat.*, 54 (2015) 2765–2776.
- [32] Y.-S. Ho, G. McKay, The kinetics of sorption of divalent metal ions onto sphagnum moss peat, *Water Res.*, 34 (2000) 735–742.
- [33] L. Ismail, H. Sallam, S.A. Farha, A. Gamal, G. Mahmoud, Adsorption behaviour of direct yellow 50 onto cotton fiber: equilibrium, kinetic and thermodynamic profile, *Spectrochim. Acta A Mol. Biomol. Spectrosc.*, 131 (2014) 657–666.
- [34] N. Oladoja, C. Aboluwoye, Y. Oladimeji, Kinetics and isotherm studies on methylene blue adsorption onto ground palm kernel coat, *Turk. J. Eng. Environ. Sci.*, 32 (2009) 303–312.
- [35] G.A. Mahmoud, E. Hegazy, N.A. Badway, K.M.M. Salam, S. Elbakery, Radiation synthesis of imprinted hydrogels for selective metal ions adsorption, *Desal. Wat. Treat.*, 57 (2016) 16540–16551.
- [36] M. Al-Ghouti, M. Khraisheh, M. Ahmad, S. Allen, Thermodynamic behaviour and the effect of temperature on the removal of dyes from aqueous solution using modified diatomite: a kinetic study, *J. Colloid Interface Sci.*, 287 (2005) 6–13.